Struct Chem (2017) 28:461–474
DOI 10.1007/s11224-016-0861-3

REVIEW ARTICLE

Green polymer chemistry: new methods of polymer synthesis using renewable starting materials

Shiro Kobayashi[1]

Received: 21 September 2016 / Accepted: 30 September 2016 / Published online: 12 November 2016

Abstract The present article reviews the recent results reported mainly from our group on "green polymer chemistry". Characteristic important aspects of green polymer chemistry include herein, typically (1) using renewable resources as starting materials for polymer production, and (2) employing green method for the polymer synthesis. As renewable starting materials, the following materials were employed; lactic acid, itaconic anhydride, renewable plant oils, and cardanol. Polymer production using these materials contributes to mitigate the carbon dioxide emission because of their "carbon neutral" nature. As green method, lipase enzyme was mainly used for polymerization catalyst, since lipase is a natural benign catalyst, showing a specific catalysis as well as recyclable character. Polymer synthesis from these materials and the catalyst provided various value-added functional polymers, demonstrating good examples of green polymer chemistry.

Keywords Green polymer chemistry · Lactic acid · Itaconic anhydride · Renewable plant oils · Cardanol · Lipase enzyme

Introduction

It has been well accepted from the beginning of the twenty-first century that environmental problems are the very important issues for maintaining the sustainable society; among others the global warming is the most serious. To mitigate the carbon dioxide emission, one of the reasons responsible for the warming, the usage of fossil feedstock's not only for energy generation but also for materials production is to be decreased. It is highly demanded, therefore, to use renewable resources as starting materials for material production. In this direction, studies on "green polymer chemistry" have very recently been conducted and reviewed in polymer production field [1–6]. It is to be noted that the concept of "green chemistry" was first noted in 1998 [7, 8], and it was extended to the polymer field as "green polymer chemistry" in the next year [9, 10]. Then, the words became used importantly [11–20]. Our studies on green polymer chemistry have been performed mostly on polymer synthesis using enzymes as catalyst ("enzymatic polymerization") and sometimes reviewed [3–6, 9, 10, 12–15, 17, 20–32].

In this article, we review with focusing on the recent developments of green polymer chemistry which have been performed mainly in our group. We conducted green polymer chemistry from two important aspects among the 12 philosophical principles [20]: (1) using renewable resources as starting materials, and (2) employing green methods for polymer synthesis.

Results and discussion

(1) Renewable resources as starting materials for polymer production

As important class of renewable resource-based starting materials for polymer production, lactic acid, itaconic acid, renewable plant oils, cardanol, etc., can be typically cited.

✉ Shiro Kobayashi
kobayash@kit.ac.jp

[1] Center for Fiber and Textile Science, Kyoto Institute of Technology, Matsugasaki, Sakyo-ku, Kyoto 606-8585, Japan

Lactic acid

Lactic acid (LA) has been a leading and most often-used starting material as renewable resource to produce polyester products [1, 3, 4, 13–16, 19]. Poly(lactic acid) (PLA) is produced in two ways; normally via ring-opening polymerization (ROP) of lactide, a six-membered cyclic dimer of LA (Scheme 1(1)) [33], and rarely via polycondensation of LA (Scheme 1(2)) [34, 35]. High molecular weight PLA was applied as a green plastics in electronic, automobile, and biomedical fields [34–45]. However, PLA involves a drawback that is susceptible to hydrolysis at the ester linkage and causes a big damage of the PLA properties (Fig. 1a), which is undesirable for the practical applications. To reduce such property damage, PLA chain is not used as a main chain but used as a side chain as shown in Fig. 1b, where the main chain is constituted from, for example, poly(alkyl methacrylate) (PRMA).

In order to prepare graft-type polymers (Fig. 1b), we employed macromonomer method as outlined in Scheme 2 [46, 47]. Reaction (1) represents the synthesis of PLA-containing methacryloyl-polymerizable macromonomer (MMm) via ROP of lactide initiated by hydroxyethyl methacrylate (HEMA). Then, MMm is radically copolymerized with various vinyl monomers like *n*-butyl methacrylate (BMA) or methyl methacrylate (MMA), giving rise to graft copolymer having PLA graft chains; PBMA-*g*-PLAm or PMMA-*g*-PLAm, where *m* means the PLA-unit number (reaction 2).

MMm macromonomers ($m = 4$, 6, 8, 12, 18, and 30) were obtained, according to the reaction (1) (Scheme 2) at 110 °C in bulk for 3 h, in high isolated yields (71–92 %) with high functionality (97–99 %). As observed interestingly in Fig. 2, T_g and T_m values (°C) of MMm were as follows; $m = 4$ (−27, –), $m = 6$ (−17, –), $m = 8$ (−12, –), $m = 12$ (−8, 58), $m = 18$ (30, 105), and $m = 30$ (38, 151), i.e., when the PLA chain length became longer, both the values increased monotonously to close to those of PLA, ~60 and ~170 °C, respectively [47].

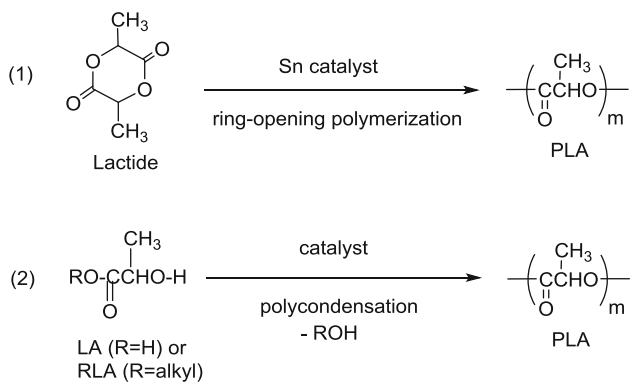

Scheme 1 PLA synthesis via **1** ROP of lactide by Sn catalyst, and **2** polycondensation of LA; R=H or alkyl group

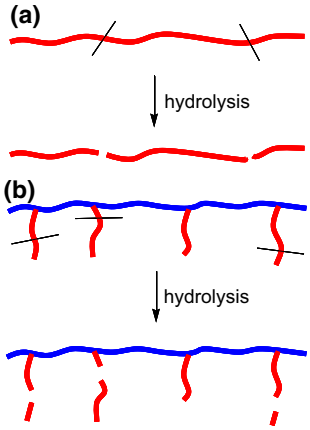

Fig. 1 **a** Polymer having PLA main chain suffers big damage of properties with hydrolysis, and **b** vinyl polymer main chain having PLA graft chains suffers less damage of properties with hydrolysis

Radical copolymerization of MMm with a vinyl monomer, reaction (2) in Scheme 2, was carried out in a miniemulsion or in an organic solvent [46, 47]. Using BMA as comonomer, MM4, MM6, and MM8 were copolymerized in the miniemulsion with using sodium dodecyl sulfate (SDS) or sodium dialkyl sulfosuccinate (PEREX) as surfactant. During the copolymerization, average particle diameter (d) became smaller, as a typical case of BMA/MM4 copolymerization from $d = 261$ nm before the polymerization to $d = 175$ nm after the polymerization, with size distribution measurement by dynamic light scattering (DLS) method. A similar tendency was observed for the other MMm copolymerization systems with BMA. These observations can be explained as follows; before the reaction the monomer droplets are present with non-covalent bond interactions, whereas after the reaction covalent bond is formed through the polymerization, causing shrinkage of the droplets. The structure of the graft copolymers was determined mainly by ^{1}H NMR analysis. The product copolymers PBMA-*g*-PLA6 from BMA/MM6 had the molecular weight M_n 12.9–16.4 × 10^4 g/mol. Physical properties of graft copolymer, e.g., PBMA-*g*-PLA6 with M_n 13.5 × 10^4 g/mol, showed T_g 37 °C, Young's modulus 1582 kgf/cm^2, tensile strength 36.7 kgf/cm^2, and elongation at break 415 %. In all copolymerization runs, the feed molar ratio of the vinyl monomer/MMm was adjusted so as to be the biomass content (PLA component for the total polymer weight) of 34 wt%.

Next, solution radical copolymerization was conducted in toluene (70 °C) or 1,4-dioxane (DOX, 60 °C) for 24 h in the combination of BMA-MMm ($m = 6$, 12, 18, and 30) or MMA-MM6 using AIBN initiator (Scheme 2, reaction 2)

Scheme 2 **1** Synthesis of MMm via ROP of lactide, and **2** synthesis of PLA-containing graft copolymer

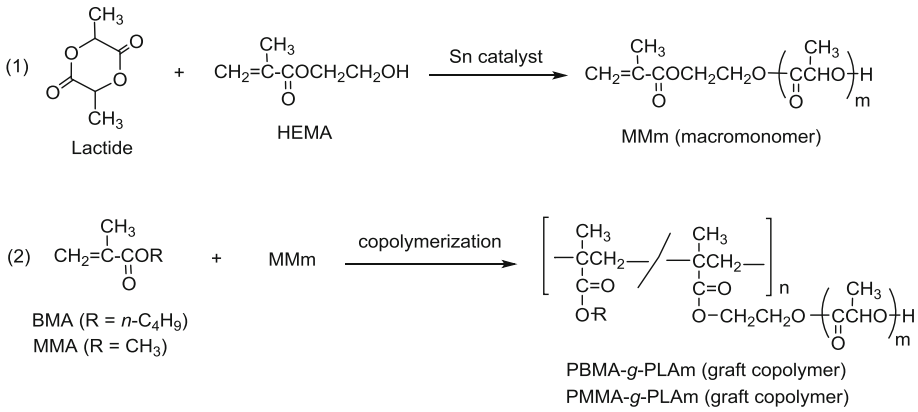

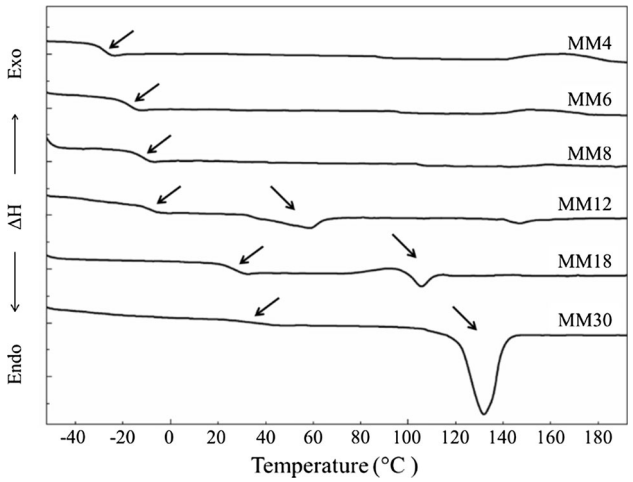

Fig. 2 DSC charts for the determination of T_g and T_m values of MMm macromonomers [47]

[47]. Various graft copolymers [PB(M)MA-*g*-PLAm] were prepared, and their properties are shown in Table 1. The reaction produced the copolymers in good to high isolated yields (54–82 %), having high M_n values ranged 2.25–6.95 × 10^4 g/mol. The copolymer composition was close to the feed monomer ratio, meaning that the monomer reactivity ratio of BMA or MMA and MMm was also close. This suggests the formation of random copolymer structure. The biomass content of the copolymers is in the range of 34–71 wt%.

It is to be noted that according to the definition of Japan BioPlastics Association proposed in 2006, "biomass plastics" denote the plastics containing the biomass content higher than 25 wt%. In this respect, all the above graft copolymers are in a context of biomass plastics.

Radical homopolymerization of MMm in DOX gave a comb polymer PMMm (Scheme 3) [47]. For the reaction to occur, a large amount of initiator AIBN of up to 10 mol % for the monomer was used. The polymer yield was relatively high in 52–81 % yields, having M_n value of the polymer 2.19–9.00 × 10^4 g/mol, which is of high molecular weight for the comb polymer. The comb polymer structure was confirmed by ^{1}H and ^{13}C NMR spectroscopy.

The polymers are all white powders and soluble materials. The DSC measurement revealed that T_g values of PMM6, PMM12, PMM18, and PMM30 are 38, 43, 50, and 58 °C, respectively. When the side chains of PLA became longer, the T_g value became higher. These results well reflect the nature of PLA chains as observed with MMm macromonomers.

Very recently, a new method of the PLA macromonomer (MMm) synthesis was developed (Scheme 4) [1]. The method is constituted from one-pot, two stages of

Table 1 Radical copolymerization of BMA or MMA with MMm to graft copolymers in an organic solvent[a] and their properties

Copolymerization in feed B(M)MA/MMm (mol/mol)	Graft copolymer					
	Structure	M_n (× 10^{-4}) (g/mol)	B(M)MA/MMm ratio in copolymer (mol/mol)	Biomass content (wt%)	T_g (°C)	Pencil hardness
BMA/MM6 (83/17)	PBMA-*g*-PLA6	2.25	82/18	34	25	<6B
BMA/MM12 (92/8)	PBMA-*g*-PLA12	5.40	92/8	34	31	<6B
BMA/MM18 (94/6)	PBMA-*g*-PLA18	3.69	95/5	34	36	3B
BMA/MM30 (83/17)	PBMA-*g*-PLA30	6.95	84/16	71	50	2B
MMA/MM6 (80/20)	PMMA-*g*-PLA6	4.90	82/18	42	67	H

[a] Toluene solvent for the upper three reactions and DOX solvent for the lower two reactions

Scheme 3 Synthesis of comb polymer

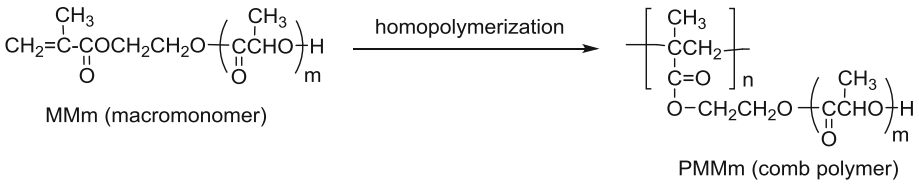

reaction. The first stage is a direct polycondensation of LA without catalyst to PLA (reaction 1), and the second stage is a ring-opening addition of PLA to glycidyl methacrylate (GMA) to afford a PLA macromonomer (GMA-Macro) (reaction 2). GMA-Macro is of analogous macromonomer MMm structure in Scheme 2 (1). Both reactions (stages 1 and 2) are performed consecutively in one-pot. This method produced GMA-Macro with high functionality in high yields. Thus, it seems the simplest and probably the cheapest way so far to prepare the PLA macromonomer. In addition, the method is metal-free, offering advantages for biomedical and pharmaceutical applications. GMA-Macro has two isomeric structures, α- and β-adducts, due to the way of ring-opening of GMA, where $\alpha{:}\beta = 30{:}70$ in approximate molar ratio (Scheme 5). However, it was shown that GMA-Macro could be similarly used for the preparation of PLA graft copolymers in solution or in miniemulsion and of PLA comb polymers in solution as described above [46, 47].

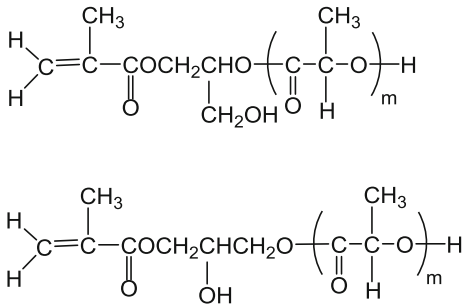

Scheme 5 α-adduct (*upper*) and β-adduct (*lower*)

Lactic acid and itaconic anhydride

Itaconic acid also belongs to a bio-based renewable resource. The other approach to PLA graft copolymer was to use a new macromonomer derived from itaconic anhydride (IAn) and LA [48]. First, ROP of lactide initiated with *n*-butyl alcohol gave PLA (reaction 1 in Scheme 6), and ring-opening addition of PLA to IAn to afford the macromonomer (IAn-PLA Macro) having a methacryloyl type polymerizable group (reaction 2 in Scheme 6) where *m* value was 5.0–12.2. Then, IAn-PLA Macro was radically copolymerized with various vinyl monomers, giving rise to PLA graft copolymers (I) (reaction 3 in Scheme 6). The copolymerization of the macromonomer with BMA was carried out in bulk or in an organic solvent (toluene or DON) to produce the graft copolymer (I) having M_n up to 1.1×10^5 g/mol. The biomass contents of the graft copolymers were 33–70 wt%. In a similar way, the copolymerization of IAn-PLA Macro with a vinyl monomer (BMA, BA, MMA, or EMA) was achieved to give the copolymers (I) in good to high yields, having biomass contents of 46–73 wt%.

Combination of IAn and PLA afforded the other new method, which is a copolymer approach [48]. First, IAn and BMA were radically copolymerized to give IAn-BMA copolymer (Scheme 7, reaction 1). The copolymers were obtained in good yields and the molecular weight M_n reaching to 1.1×10^5 g/mol having IAn:BMA = 1.0:5.8 (molar ratio). Then, grafting the PLA chain onto IAn-BMA copolymer was performed by Sn-catalyzed reaction of PLA

Scheme 4 One-pot two-stage synthesis of macromonomer (GMA-Macro): **1** synthesis of poly(lactic acid) (PLA) directly from lactic acid (LA) and **2** ring-opening addition between glycidyl methacrylate (GMA) and PLA

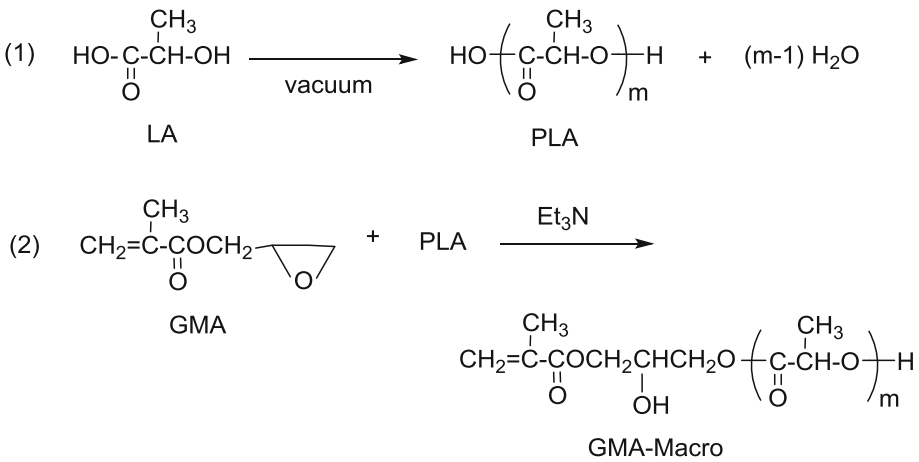

Scheme 6 Synthesis of IAn-PLA Macro and PLA-Graft copolymer (I)

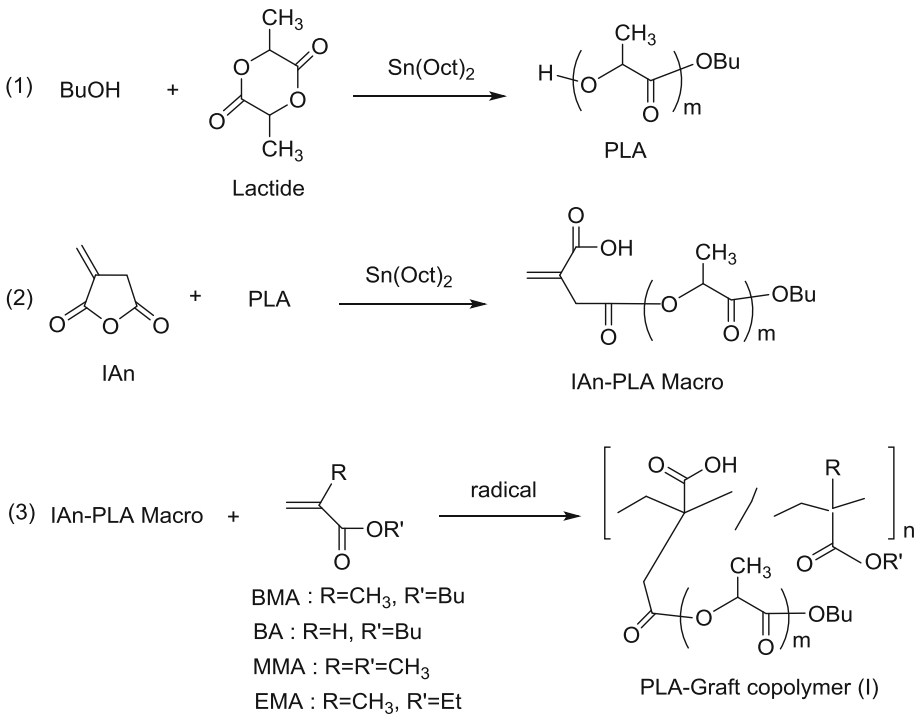

to afford PLA graft copolymer (II) via reaction (2). The copolymer yield was moderate, which was partly due to the difficulty of the complete separation of the starting PLA and the product graft copolymer. The M_n value 5.76×10^4 g/mol was little increased to 5.88×10^4 g/mol after the grafting. The molar ratio of the copolymer, PLA (grafted):IAn:BMA = 0.33:0.67:2.9, revealed the biomass content of 35 wt%, which belongs to a biomass plastics.

Lactic acid and polyol for star-shaped oligomer

Multi-functional star-shaped oligo(lactic acid)s (oligoLAs) with reactive double bonds were synthesized from the oligoLA polyols. They were applied to bio-based curable coatings. The synthesis procedure is shown in Scheme 8, using pentaerythritol as a polyol [49, 50].

The molecular weight of the star-shaped oligoLA polyol ($l + m + n + o = 14$) was obtained by GPC as $M_n = 1400$ g/mol with $M_w/M_n = 1.4$ (reaction 1). The polyol was amorphous by DSC analysis and had about 88 % biomass content. It was applied to use as test coatings on the grip part of TOYOTA personal mobility "i-REAL"; the coating was conducted via two-component thermal curing with mixing the polyol and a polyisocyanate hardener [49]. The biomass content of the cured coatings was 40 wt%.

The product, star-shaped oligoLA modified with glycidyl methacrylate (S-OLAM-1) according to reaction (2),

Scheme 7 Copolymer approach

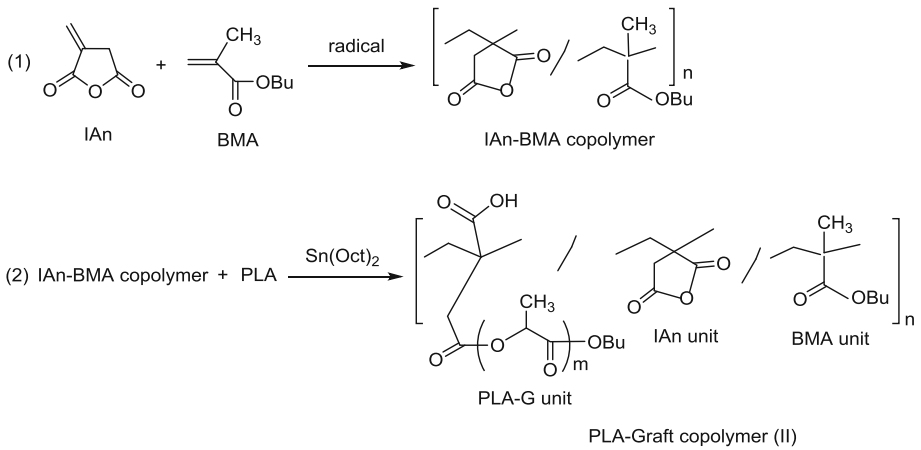

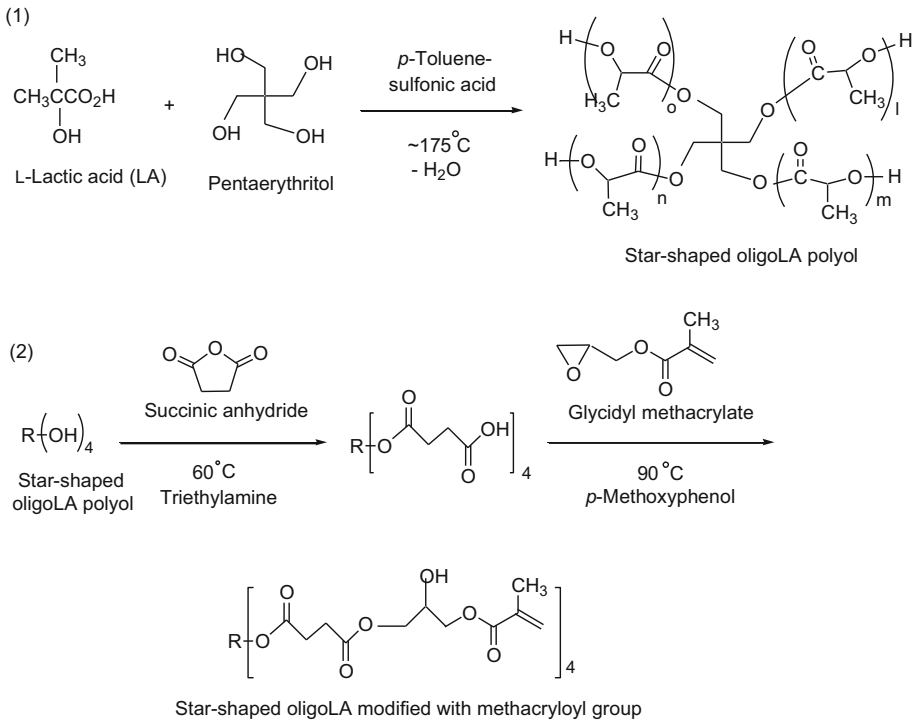

Scheme 8 1 Synthesis of star-shaped oligoLA polyol from LA and pentaerythritol, and **2** synthesis of star-shaped oligoLA modified with methacryloyl group (S-OLAM-1) from the polyol, succinic anhydride, and glycidyl methacrylate

was of $M_n = 2600$ g/mol with $M_w/M_n = 1.3$ with average 4.6 methacryloyl groups per molecule, having biomass content 41 wt% (63 wt% when succinic anhydride accounted as biomass). Instead of pentaerythritol, dipentaerythritol also gave another S-OLAM-2. These S-OLAM-1 and -2 were applied for UV curable coatings. For example, formulation was a mixture of S-OLAM-2 (70 wt%), urethane hexaacrylate (30 wt%), and a photo-initiator (5 wt%). The coating film was prepared by air spray coatings on polycarbonate, and the film was irradiated by mercury lamp, forming the cured film, whose thickness was 15 μm. Some performance data of the UV-cured coating film were all good for initial adhesion, humidity resistance, alkaline resistance, and abrasion resistance. Pencil hardness of the cured film was F, and the biomass content of the film was 29 wt% (44 wt% when succinic anhydride taken into account), showing "biomass plastics" for the film [49, 50].

Pendant lactic acid chain for polyol

For improvement of anti-hydrolysis performance as shown in Fig. 1, humidity resistance of cured coating films (AP-PLA, Scheme 9) of acrylic polyols (AP) with pendant PLA chains was examined [51]. AP-PLA was prepared via radical copolymerization of HEMA, *n*-butyl acrylate (nBA), and PLA macromonomer derived from HEMA (Scheme 2) [46, 47]. By varying the feed monomer ratio, the AP-PLA was prepared: The M_w of the polymer was about 10,000–20,000 g/mol with M_n around 3200–10,000 g/mol. The hydrolysis behavior of the coating films prepared from the cured AP-PLA with polyisocyanate was evaluated. It was found that the 51 wt% bio-content coating satisfied the basic coating performances when HEMA was copolymerized and total OH value was more than 120 mg KOH/g. These results demonstrate that the PLA macromonomers derived from lactic acid are useful for good coating materials [51].

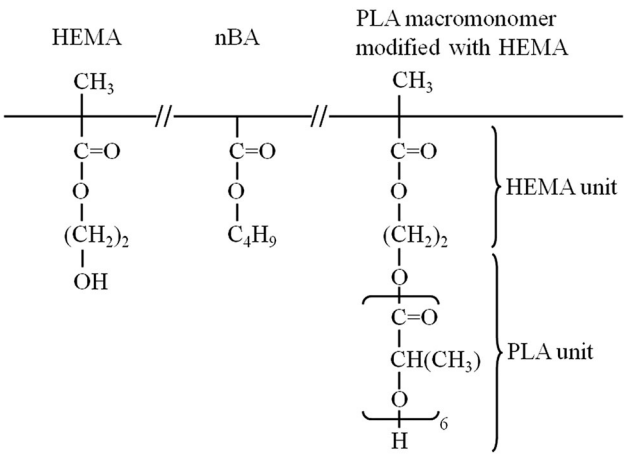

Scheme 9 Model structure of AP-PLA

Lactic acid and renewable oil

Castor oil, a renewable plant oil, having branched poly(L-lactic acid) (PLLA) chain was synthesized by ring-opening polymerization of lactide using castor oil as an initiator [52]. The structure of the branched polymer is shown in Scheme 10. The molecular weight of the branched polymer increased linearly as a function of the feed ratio of lactide and castor oil. The thermal properties of the branched polymer were compared with those of linear PLLA. When a blended film of the branched polymer and a net PLLA were compared, a content of 5 wt% of the branched polymer was sufficient to increase the strain at break, due to the nature of plasticizing PLLA. Thermomechanical analysis of the blended film revealed a decrease in the initial elastic modulus with addition of the branched polymer. T_g and T_m values increased as a function of the feed ratio, and these values were lower for the branched polymer than for PLLA [52].

Renewable plant oil (organic)–inorganic hybrid material: green nanocomposite

Green clay-nanocomposites from plant oil derivatives were prepared for the first time [53]. The *green nanocomposites* are consisting of the abundant inexpensive natural resources, plant oils, and clay. An epoxidized triglyceride oil, epoxidized soybean oil (ESO, Scheme 11), was subjected to intercalation into an organically modified clay, octadecyl-modified montmorillonite 8 (OMM), by an acid-catalyzed curing of ESO at 150 °C, leading to production of a new class of biodegradable nanocomposites. The nanocomposite, having OMM content of 5, 10, 15 or 20 %, has the homogeneous structure of organic and inorganic components, in which silicate layers of the clay were intercalated and randomly distributed in the polymer matrix. T_g of the nanocomposite increased from −2 to 4 °C with increasing clay content from 5 to 15 %, which may be due to a decrease in mobility of the cross-linked polymer chain by silicate layers. The reinforcement effect by the addition of the clay was confirmed by dynamic viscoelasticity analysis. Interestingly, the nanocomposite exhibited flexible property as seen in Fig. 3 [53].

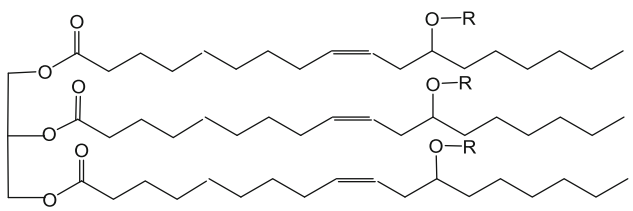

Scheme 10 Structure of castor oil (R=H) and LA chain-branched castor oil (R=−[C(=O)CH(CH_3)O]$_m$−H, *m*; variable)

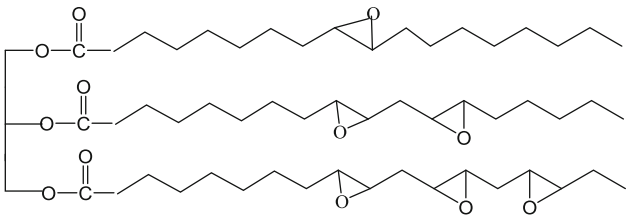

Scheme 11 Structure of ESO

The above results were extended: epoxidized soybean oil (ESO) and epoxidized linseed oil (ELO) were used as an organic monomer [54]. Montmorillonite was modified by dodecylamine, octadecylamine, and 12-aminododecanoic acid to give three organophilic clays (C_{12}-Mont, C_{18}-Mont, and $C_{11}CO_2H$Mont, respectively). The hybrid was synthesized by curing the epoxidized oil using a thermally latent cationic catalyst in the presence of the organophilic clay at 150 °C for 2 h. These nanocomposites showed high thermal stability and mechanical properties superior to those of the corresponding oil polymers due to the reinforcement effect by the clay particles, but the little reduced flexibility due to the intercalation (Table 2) [54].

In addition, not only ESO and ELO but epoxidized fish oil (EFO) were employed for the green nanocomponent production [55]. The ESO-OMM nanocomposite containing 20 % clay was treated at 900 °C in air, giving rise to porous ceramics with platelet structure.

Green nanocomposite coatings based on renewable plant oils were also developed. An acid-catalyzed curing of ESO

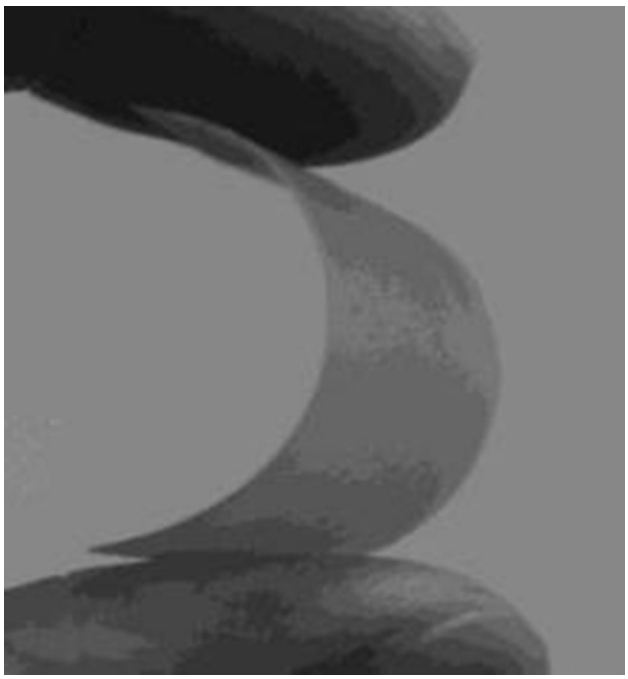

Fig. 3 Photograph of ESO-clay nanocomposite showing high flexibility

Table 2 Mechanical properties of ESO–$C_{11}CO_2H$Mont hybrids

Clay content (%)	Tensile modulus (MPa)	Tensile strength (MPa)	Elongation at break (%)
0	11	1.4	16
2	18	1.8	14
5	22	2.0	12
10	33	3.4	13

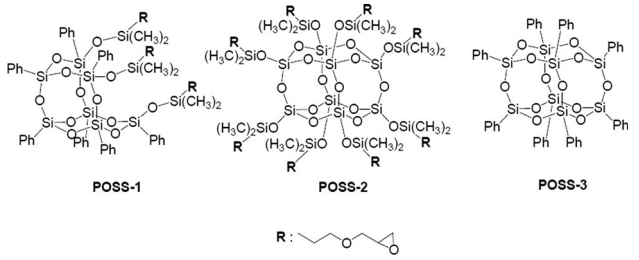

Fig. 4 Structures of POSS employed [58]

(Scheme 11) with a silane compound, 3-glycidoxypropyltrimethoxysilane (GPTMS), produced transparent nanocomposites. The covalent linkage between the organic and inorganic polymers probably controls the nanocomposite structure in nanoscales, leading to improvement of coating properties. The nanocomposite exhibited excellent film properties. The hardness and mechanical strength improved by incorporating the silica network into the organic polymer matrix, and good flexibility was observed in the nanocomposite. The nanocomposite showed high biodegradability [56]. Similar results were observed by using a silane coupling agent instead of GPTMS to give a transparent and highly glossy green nanocomposite [57].

Green nanocomposites based on renewable plant oils and polyhedral oligomeric silsesquioxanes (POSS, Fig. 4) were developed, where epoxidized soybean and linseed oils (ESO and ELO, respectively) were used for the plant oil components [58]. An acid-catalyzed curing of ESO or ELO with oxirane-containing POSS derivatives at 140 °C for 2 h produced transparent nanocomposite coatings with high gloss surface, in which the organic and inorganic components were linked via covalent bonds via ring-opening addition reaction of oxirane groups to form the network structure. The resulting nanocomposites were insoluble for common organic solvents and water.

The hardness and mechanical strength were improved by the incorporation of the POSS unit into the organic polymer matrix (Table 3). In both cases of ESO and FLO, the hardness and Young's modulus values were much increased by incorporating POSS-1 or -2. W_e/W_{tot} can be regarded as elasticity, and the value decreased with addition of POSS as seen in Table 3, probably due to the cross-linking of the organic polymer parts. Nanostructural analyses of the nanocomposites showed the formation of homogeneous structures at the micrometer scale. The study demonstrated the correlation between the nanostructure of composites and macroscopic properties [58].

It is to be noted that in the above studies on *green nanocomposites*, the nanocomposites are produced from inexpensive renewable resources including plant oils and exhibited good biodegradability, contributing to global sustainability.

Cardanol for artificial urushi

Cardanol is a major component obtained from cashew nut shell liquid, and hence, it is a typical renewable resource. It has a structure close to natural urushiol, which gives traditional Japanese lacquer "Urushi" via laccase-catalyzed oxidative polymerization in air; urushiol has a catechol structure (Scheme 12), whereas cardanol possesses a phenol structure (Scheme 13), both having a saturated or unsaturated C_{15} hydrocarbon chain with one, two or three double bonds. Recent years, production of urushi sap from urushi trees much decreased in Japan, and therefore natural urushi became very expensive; natural urushi nowadays is employed only in limited area, like the fine arts. We regarded cardanol as an urushiol analog monomer, which was polymerized by an enzyme or a transition metal catalyst [3, 15]. We studied developing "artificial urushi" from cardanol, which is much cheaper yet with hoping that it could be used in place of natural urushi for commodity use [59–62]. The cardanol polymerizations were carried out using Fe–salen as an enzyme model catalyst under various reaction conditions in an organic solvent [59, 62], or in bulk [61]. These polymerizations, however, involve undesirable situations; the polymerization using an organic solvent is not desirable from the green viewpoint and the bulk system induced undesirable exothermic reaction to yield a little insoluble or unstable prepolymer.

Natural urushi sap is known to polymerized in a water-in-oil (w/o, water-in-urushiol) emulsion system to give urushiol prepolymer and eventually natural urushi; the urushi sap is composed of urushiol (55–70 %), water-soluble polysaccharides (6–10 %), glycol-proteins (1–3 %), laccase enzyme (<1 %), and water (20–30 %) [63, 64]. We considered that when the cardanol polymerization could be achieved in a water-in-cardanol (w/o) emulsion, the above undesirable situations would be solved or much reduced. Then, we challenged the emulsion polymerization of

Table 3 Film properties of green nanocomposites

Entry	Epoxidized plant oil	POSS[a]	Pencil scratch hardness	Universal hardness[b] ($N \cdot mm^{-2}$)	Young's modulus[b] (MPa)	$W_e/W_{tot}^{b,c}$ (%)
1	ESO	–[d]	2B	9	210	90
2	ESO	1 (10)	2H	16	450	78
3	ESO	2 (10)	4H	23	700	68
4	ELO	–[d]	2H	47	1190	45
5	ELO	1 (10)	5H	49	1620	39
6	ELO	2 (10)	> 6H	55	1760	42

[a] In parenthesis: amount of POSS (wt%)

[b] Determined by microhardness tester

[c] W_e work volume of elastic deformation, W_{tot} total work volume

[d] No additive

Scheme 12 Natural urushi is formed via two-stage reactions involving laccase-catalyzed oxidation polymerization of urushiol to give prepolymer and it's curing

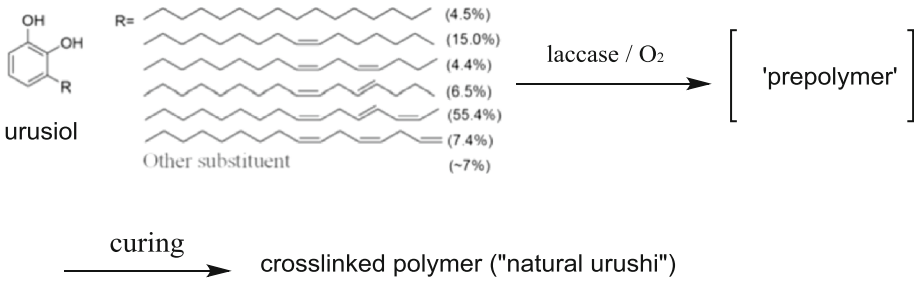

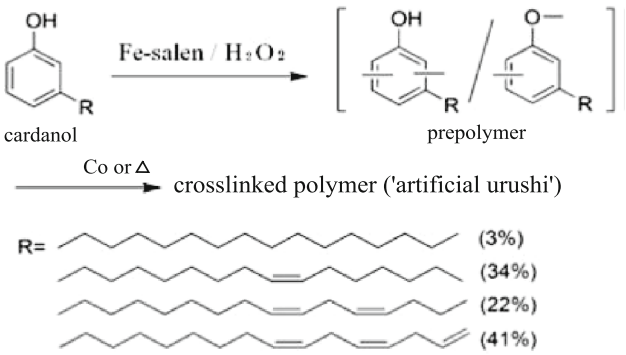

Scheme 13 Synthesis of artificial urushi via two-stage reactions involving Fe–salen catalyzed oxidation polymerization of cardanol to give prepolymer and it's cross-linking

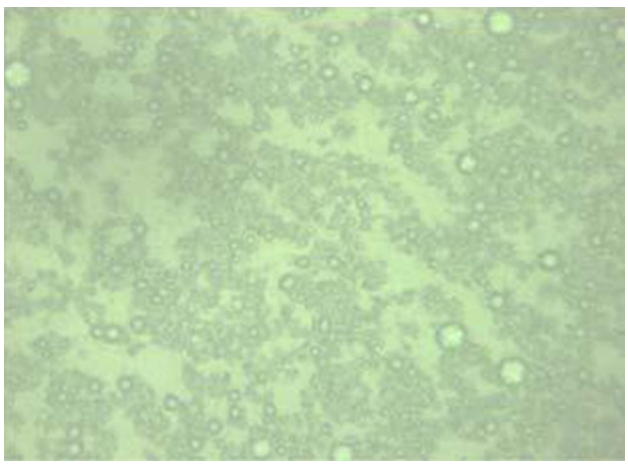

Fig. 5 Optical micrograph of the w/o emulsion: water/cardanol (33/67) mixture containing PEI/AA/Fe–salen

cardanol, which is a new biomimetic oxidative polymerization of cardanol, leading to artificial urushi [64].

First, it was most important to find out the w/o emulsion system for the cardanol polymerization. Then, it was disclosed that combination of an oligo- to poly-amine and a weak acid like acetic acid (AA) served as an efficient emulsifier for the polymerization. Figure 5 shows an optical micrograph of the w/o emulsion before the polymerization, where the size of water droplets is ~ 15 μm. It is to be noted that natural urushi sap showed a similar optical micrograph of a w/o emulsion [64]. As a typical polymerization, to a w/o emulsion mixture of water (0.60 g), cardanol (0.60 g, 2.0 mmol), polyethyleneimine (PEI1800, mol wt = 1800 g/mol, 6.0 mg), and AA (8.4 mg, equimolar to amino-groups of PEI), 30 % H_2O_2 (80 μL, 0.71 mmol) was added dropwise ten times under stirring for 2 h at 20 °C, and then the reaction mixture was further stirred for 24 h. The viscous oily product of prepolymer was obtained; conversion of monomer 50 % with M_n 5600 g/mol. After the polymerization, the prepolymer

solution kept the emulsion situation and exhibited a good film formation property. The coated films were cured thermally or by Co-naphthenate-catalyzed cross-linking reaction, e.g., the thermally cured film at 150 °C for 1 h showed the pencil hardness of 4H [64]. Thus, we could mimic the natural urushi system involving the w/o emulsion by using cardanol starting material, in aiming to develop artificial urushi.

(2) Green methods for polymer synthesis

We have been studying extensively on the polymer synthesis employing enzymes as green catalyst [2–5, 9, 10, 12–15, 17, 20–32]. Among six classes of enzymes, the following three classes have been used for the polymer synthesis; (1) oxidoreductases (peroxidase, laccase, tyrosinase, glucose oxidase, etc.), (2) transferases (phosphorylase, glycosyltransferase, acyltransferase, etc.), and (3) hydrolases (glycosidases [cellulase, amylase, xylanase, chitinase, hyaluronidase, etc.], lipase, protease, peptidase, etc.).

Lipase catalysis

Among the enzymes, lipase is one of the most extensively studied, which actually initiated the enzymatic polymerization thorough using it for the catalyst of ring-opening polymerization of cyclic esters (lactones) in 1993 [65–67]. Lipase-catalyzed polyester synthesis has also been reviewed [3, 4, 10, 12–15, 17, 19, 20, 22, 23, 26, 27, 29, 31, 32]. In this paper, we focus on the lipase-catalyzed polymerization for the substrate monomers derived from renewable starting materials.

Itaconic anhydride (IAn) as a lactone derivative was subjected to lipase catalysis, leading to reactive polyesters [2]. Lipase-catalyzed ring-opening addition condensation polymerization (ROACP) involving dehydration was reported to produce polyesters from carboxylic acid anhydride like succinic anhydride (SAn) or glutaric anhydride (GAn) and a diol [68]. ROACP of IAn and a diol, however, did not give an expected polyester. But, ROACP reaction of three components, IAn, SAn, or GAn, and a diol at 25 °C in toluene produced reactive polyesters in good to high yields (Scheme 14) [2]. From SAn, the polyesters with M_n values 650–3510 g/mol, and with numbers of unit per molecule values 1.3–2.6 were obtained. From GAn, the corresponding values were 560–3690 g/mol and 1.2–3.1, respectively. Cross-linking reaction of a product polyester showed reactive nature, giving a cross-linked hard solid polyester. These polyesters derived from renewable starting materials suggested possible applications for macromonomer, telechelics, or cross-linking reagent, and the vinylidene group(s) could be utilized for further modifications.

A specific lipase catalysis was disclosed in the oligomerization of alkyl lactates. Lipase (Novozym 435)-catalyzed polycondensation of alkyl D-lactates (RDLa, an oxyacid ester) at 50 °C gave oligo(D-lactic acid)s (oligoDLAs) up to 82 % yields with n value = 2–7 (Scheme 15) [69]. Primary alkyl lactates of Et-, Pr-, and Bu- showed a higher reactivity than longer alkyl lactates like Pe-, Hx-, Hp-, and Oc-, and a secondary alkyl lactate of sBuDLa showed a decreased reactivity. On the other hand, L-lactates did not show any reactivity, i.e., enantioselection for D-isomers is very strict.

Michaelis–Menten Eq. (1) and a pseudo-first-order rate Eq. (2) were applied for the reaction analysis,

$$\mathrm{E} + \mathrm{S} \underset{}{\overset{k'}{\rightleftarrows}} \mathrm{ES} \xrightarrow{k_{\mathrm{cat}}} \mathrm{P} + \mathrm{E} \tag{1}$$

$$-\frac{\mathrm{d}[\mathrm{S}]}{\mathrm{dt}} = k'[\mathrm{E}][\mathrm{S}] = k[\mathrm{S}] \quad (k'[\mathrm{E}] = k) \tag{2}$$

where E, S, and P denote enzyme, substrate, and product, respectively. Plots of integrated form of Eq. (2) gave k values ($\times 10^4$ s^{-1}): MeDLa (3.7); EtDLa (4.4); PrDLa (3.7); and BuDLa (3.4).

For examining the inhibition function of EtLLa for the oligomerization of EtDLa, EtLLa was added to the EtDLa reaction. The reaction rate, namely the EtDLa consumption rate (v_0, mol L^{-1} s^{-1}), was evaluated, and the values were plotted according to Lineweaver–Burk plots. The plots showed that an inhibition type of EtLLa on the

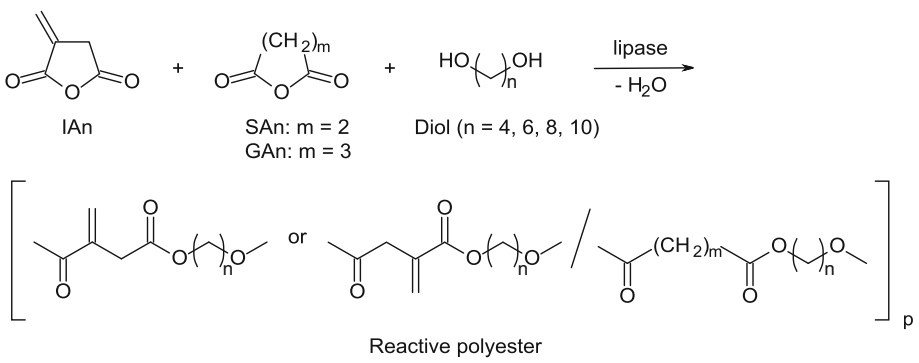

Scheme 14 Lipase-catalyzed ROACP between IAn, SAn or GAn, and a diol

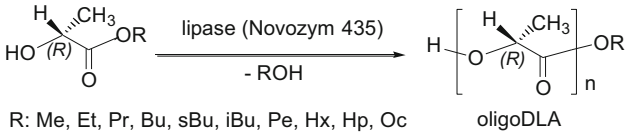

Scheme 15 Enantioselective oligomerization of D-alkyl lactates

oligomerization of EtDLa is "competitive". From the plots, the Michaelis constant $K_m = 2.35$ (mol L^{-1}) and the maximum rate $V_{max} = 1.48 \times 10^{-3}$ (mol L^{-1} s^{-1}) were obtained.

Hydrolysis of BuDLa and BuLLa was conducted in THF at 50 °C (Scheme 16) [69]. In contrast to the oligomerization, Novozym 435-catalysis induced the hydrolysis of both BuDLa and BuLLa substrates, although BuDLa was consumed faster than BuLLa. The rough values ($\times 10^4$ L mol^{-1} s^{-1}) are $k = 2.1$ for BuDLa and $k = 0.92$ for BuLLa; the D-isomer proceeded about 2.3 times faster than the L-isomer.

These observations suggested the mechanistic aspects of lipase (Novozym 435) catalysis: enantioselection is operated by deacylation step as given in Scheme 17 [69], where for simplicity only dimer formation is shown. At first, the D-lactate monomer (substrate) is to be activated by enzyme with forming *(R)*-acyl-enzyme intermediate in step (a), (enzyme-activated monomer: **EM**), ("acylation of lipase") shown in (A). Onto the activated carbonyl carbon of **EM**, OH-group of the D-lactate nucleophilically attacks to form an ester bond with liberating lipase enzyme, giving rise to D,D-dimer in step (b) ("deacylation of lipase"). When, in place of the D-lactate monomer, OH-group of D,D-dimer attacks **EM**, D,D,D-trimer will be formed, and the repetition of this type of reaction ends up with the formation of higher D-oligomers. Since the L-lactate was not consumed, the reaction of **EM** with OH-group of L-lactate does not occur; reaction of step (c) does not take place. On the other hand, hydrolysis of D-lactate also needs activation to form **EM**. Then, EM reacts with water to give D-lactic acid shown in step (d).

In the reactions of L-lactate monomers (B), alkyl L-lactates were not consumed in the oligomerization. While, in the hydrolysis, alkyl L-lactates were hydrolyzed to give L-lactic acid in step (h). This is a clear indication that step (e) actually took place to produce *(S)*-acyl-enzyme intermediate **EM**. However, neither OH-group of D-lactate nor OH-group of L-lactate was allowed to attack **EM** to give L,D-dimer via step (f) or L,L-dimer via step (g).

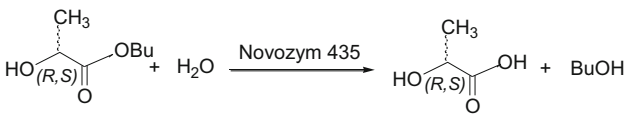

Scheme 16 Lipase-catalyzed hydrolysis of BuDLa and BuLLa

Although hydrolysis steps (d) and (h) (both deacylations) are non-selective due to no chirality in water molecule, esterification steps (b), (c), (f), and (g) (all deacylations) are enantioselective. The above results demonstrate that "the enantioselection is governed by the deacylation step"; among four steps, only step (b) was allowed to give D,D-dimer. The **EM** formation, both steps (a) and (e), was possible, however, from all alkyl D- and L-lactate monomers.

For comparison, protease catalysis was examined, which is known to hydrolyze proteins for L-amino acid residues. Proteases were therefore employed with expectation to cause L-enantioselective oligomerization of alkyl D- and L-lactates (RDLa and RLLa), in contrast to the lipase (Novozym 435)-catalyzed perfect D-enantioselective reaction in Scheme 17. The examined four proteases gave preferentially oligo(L-lactic acid)s (oligoLLAs; dimer–pentamer), with moderate to high yields. The enantioselection was in L-/D-selective ratio; 56/28–25/4 in conversion % ratio, showing an opposite direction in enantioselection of the lipase as expected, but not strictly [70]. Hydrolysis reaction of ethyl D- and L-lactates (EtLa)s catalyzed by protease took place; EtLLa was consumed little faster than EtDLa. The mechanism of the protease-catalyzed oligomerization was explained similarly to that of lipase as seen in Scheme 17, but with the L-selective manner; the enantioselection is governed by the deacylation step.

It is to be mentioned that the above D-selective reaction of alkyl lactates by lipase catalysis was applied for optical resolution of D, L-isomers [71]. Also, degradation of polyester by lipase catalyst can be a possible green method of polymer recycling [11].

Finally, we add here a very unique catalysis of lipase: "dehydration reaction is catalyzed by lipase in water", because water as solvent is a part of green polymer chemistry [72, 73]. A dehydration reaction is generally conducted in nonaqueous media. Since the product water of the dehydration is in equilibrium with starting materials, the solvent water disfavors the dehydration to proceed in an aqueous medium due to the "law of mass action". Nevertheless, lipase catalysis enabled a dehydration polycondensation of a dicarboxylic acid and a glycol in water at 45 °C to afford a polyester in good yields (Scheme 18) [72, 73]. In the polymerization of an α,ω-dicarboxylic acid and a glycol, the polymerization behavior was greatly depending on the methylene chain length of the monomers (reaction 1). For example, lipases CA and lipase PC were active for polycondensation of sebacic acid ($m = 8$) and 1,8-octanediol to give polyester with $M_n \sim 1600$ g/mol in up to 50 % yields. The polymer was obtained in good yields from 1,10-decanediol, whereas no polymer formation was observed from 1,6-hexanediol, suggesting that the combination of the monomers with appropriate hydrophobicity is

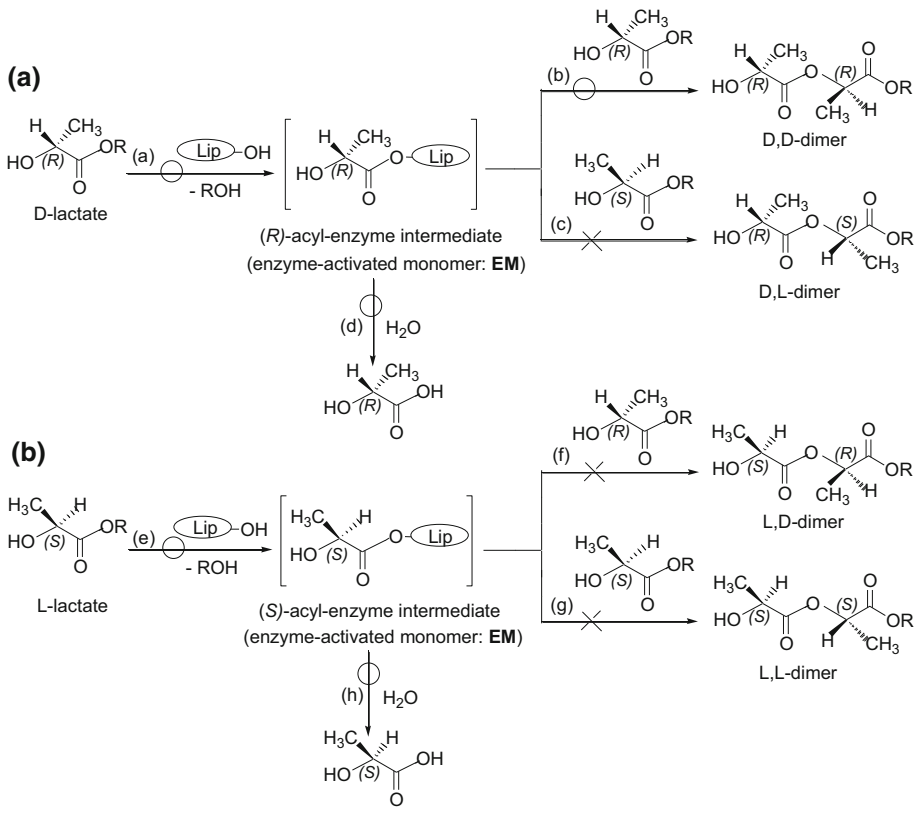

Scheme 17 Lipase-catalyzed reaction pathways of D-lactates **A** and L-lactates **B:** acyl-enzyme intermediate formation steps (a and e), subsequent dimer formation steps (*b*, *c*, *f*, and *g*), and hydrolysis steps (*d* and *h*). *Open circle* denotes that the step takes place, whereas × denotes that the step does not take place. (In steps *b*–*d*, *f*–*h*, the leaving group of lipase is omitted.)

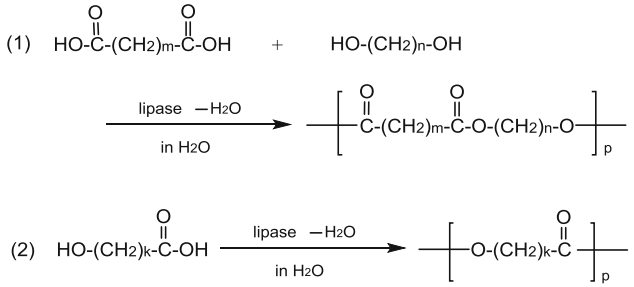

Scheme 18 Lipase-catalyzed dehydration polymerization in water solvent to produce polyester: **1** from dicarboxylic acid and glycol, and **2** from oxyacid

required for the polymer production by dehydration. Similar tendency was observed in the dehydration polymerization of oxyacids; from an oxyacid ($k = 11$ or 14) polyester around M_n 1000 g/mol was obtained in up to 59 % yields (reaction 2). It should be stressed that this finding of the dehydration reaction in water is a new aspect in organic chemistry.

Conclusion

The climate change of global warming is increasingly serious in the new century. For us polymer scientists, it is highly demanded to conduct green polymer chemistry to contribute to the problem with mitigating the carbon dioxide emission. In this article, we have focused on the results conducted from this direction mostly in our group, dealing with (1) using renewable resources as starting materials for polymer production, and (2) employing green catalyst for polymer synthesis, including the finding of a new reaction like dehydration in water solvent. These results suggest future possible ways to be conducted for green polymer chemistry.

Lastly we wish to send to Prof. G. A. Olah: Many congratulations for the 90th birthday!

Acknowledgments The present author wishes to thank all the coauthors referred in this article for their enthusiastic collaborations in pursuing the research work.

References

1. Yoshimura Y, Nojiri M, Arimoto M, Ishimoto K, Aso Y, Ohara H, Yamane H, Kobayashi S (2016) Green polymer chemistry: one-pot, metal-free synthesis of macromonomer via direct polycondensation of lactic acid and its radical polymerization to graft and comb polymers. Polymer 90:342–350
2. Yamaguchi S, Tanha M, Hult A, Okuda T, Ohara H, Kobayashi S (2014) Green polymer chemistry: lipase-catalyzed synthesis of bio-based reactive polyesters employing itaconic anhydride as a renewable monomer. Polym J 46:2–13
3. Shoda S, Uyama H, Kadokawa J, Kimura S, Kobayashi S (2016) Enzymes as green catalyst for precision macromolecular synthesis. Chem Rev 116:2307–2413

4. Kobayashi S (2015) Enzymatic ring-opening polymerization and polycondensation for the green synthesis of polyesters. Polym Adv Technol 26:677–686
5. Shoda S, Kobayashi A, Kobayashi S (2015) Production of polymers by white biotechnology. In: Coelho MAZ, Ribeiro BD (eds) White biotechnology for sustainable chemistry. R Soc Chem, UK, pp 274–309
6. Coleen P, Liu T, Yan J, Kobayashi S (2015) Enzymatic polymerizations. In: Kobayashi S, Muellen M (eds) Encyclopedia of polymeric nanomaterials, Springer, Berlin
7. Anastas PT, Warner JC (1998) Green chemistry: theory and practice. Oxford University Press, Oxford
8. Vorvath IT, Anastas PT (2007) Innovations and green chemistry. Chem Rev 107:2169–2173
9. Kobayashi S (1999) Enzymatic polymerization–polymer synthesis catalyzed by a natural macromolecule. High Polym Jpn 48:124–127
10. Kobayashi S (1999) Enzymatic polymerization: a new method of polymer synthesis. J Polym Sci Part A: Polym Chem 37:3041–3056
11. Kobayashi S, Uyama H, Takamoto T (2000) Lipase-catalyzed degradation of polyesters in organic solvents. A new methodology of polymer recycling using enzyme as catalyst. Biomacromolecules 1:3–5
12. Kobayashi S, Uyama H, Kimura S (2001) Enzymatic polymerization. Chem Rev 101:3793–3818
13. Kobayashi S, Uyama H, Ohmae M (2001) Enzymatic polymerization for precision polymer synthesis. Bull Chem Soc Jpn 74:613–635
14. Kobayashi S (2009) Recent developments in lipase-catalyzed synthesis of polyesters. Macromol Rapid Commun 30:237–266
15. Kobayashi S, Makino A (2009) Enzymatic polymer synthesis: an opportunity for green polymer chemistry. Chem Rev 109:5288–5353
16. Puskas JE, Sen MY, Seo KS (2009) Green polymer chemistry using nature's catalyst, enzyme. J Polym Sci Part A: Polym Chem 47:2959–2976
17. Kobayashi S (2010) Lipase-catalyzed polyester synthesis—a green polymer chemistry. Proc Jpn Acad Ser B 86:338–365
18. Kobayashi S (2011) Green polymer synthesis using enzyme catalysts. In: Misono M, Murahashi S (eds) Green chemistry—chemistry for sustainable society. Kodansha Scientific, Tokyo, pp 192–203
19. Cheng HN, Gross RA (eds) (2011) Green polymer chemistry: biocatalysis and biomaterials, ACS Symposium Ser 1043
20. Kobayashi S (2013) Green polymer chemistry: recent developments. Adv Polym Sci 262:141–166
21. Uyama H, Kobayashi S (1999) Enzymatic polymerization yields useful polyphenols. Chem Tech 29:22–28
22. Kobayashi S, Uyama H (2001) In vitro biosynthesis of polyesters. In: Babel W, Steinbüchel A (eds) Advances in biochemical engineering/biotechnology, vol 71, biopolyesters. Springer, Heidelberg, pp 241–262
23. Kobayashi S, Uyama H (2002) In vitro polyester synthesis via enzymatic polymerization. Curr Org Chem 6:209–222
24. Kobayashi S, Higashimura H (2003) Oxidative polymerization of phenols revisited. Prog Polym Sci 28:1015–1048
25. Uyama H, Kobayashi S (2003) Enzymatic synthesis of polyphenols. Curr Org Chem 7:1387–1397
26. Kobayashi S, Uyama H (2003) Enzymatic polymerization. In: Kroschwitz JI (ed) Encyclopedia of polymer science and technology, vol 2, 3rd edn. Wiley, New York, pp 328–364
27. Kobayashi S, Ritter H, Kaplan D (eds) (2006) Enzyme-catalyzed synthesis of polymers. Adv Polym Sci (special issue), vol 194
28. Kobayashi S (2007) New developments of polysaccharide synthesis via enzymatic polymerization. Proc Jpn Acad Ser B 83:215–247
29. Kobayashi S, Ohmae M (2007) Polymer synthesis and modification by enzymatic catalysis, In: Matyjasjewski K, Gnanou Y, Leibler L (eds) Macromolecular engineering: precise synthesis, materials properties, applications. vol 1: Synthetic techniques, Chapter 10, Wiley, Weinheim, pp 401–477
30. Kadokawa J, Kobayashi S (2010) Polymer synthesis by enzymatic catalysis. Curr Opin Chem Biol 14:145–153
31. Kobayashi S (2012) Enzymatic polymerization. In: Matyjaszewski K, Moeller N (eds) Polymer science: a comprehensive reference, vol 5. Elsevier, Amsterdam, pp 217–237
32. Kobayashi S (2014) Enzymatic polymerization. In: Seidel A (ed) Encyclopedia of polymer science and technology, vol 5, 4th edn. Wiley, Hoboken, pp 221–292
33. Dechy-Cabaret O, Martin-Vaca B, Bourissou D (2004) Controlled ring-opening polymerization of lactide and glycolide. Chem Rev 104:6147–6176
34. Moon SI, Lee CW, Miyamoto M, Kimura Y (2000) Melt polycondensation of L-lactic acid with Sn(II) catalysts activated by various proton acids: a direct manufacturing route to high molecular weight poly(L-lactic acid). J Polym Sci Part A: Polym Chem 38:1673–1679
35. Moon SI, Lee CW, Taniguchi I, Miyamoto M, Kimura Y (2001) Melt/solid polycondensation of L-lactic acid: an alternative route to poly(L-lactic acid) with high molecular weight. Polymer 42:5059–5062
36. Tsuji H, Ikada Y (2000) Properties and morphology of poly(L-lactide) 4. Effects of structural parameters on long-term hydrolysis of poly(L-lactide) in phosphate-buffered solution. Polym Deg Stab 67:179–189
37. Gupta B, Revagade N, Hilborn J (2007) Poly(lactic acid) fiber: an overview. Prog Polym Sci 32:455–482
38. Fukushima K, Chang YH, Kimura Y (2007) Enhanced stereocomplex formation of poly(L-lactic acid) and poly(D-lactic acid) in the presence of stereoblock poly(L-lactic acid). Macromol Biosci 7:829–835
39. Jiang X, Smith MR III, Baker GL (2008) Water-soluble thermoresponsive polylactides. Macromolecules 41:318–324
40. Jing F, Hillmyer MA (2008) A bifunctional monomer derived from lactide for toughening polylactide. J Am Chem Soc 130:13826–13827
41. Inkinen S, Hakkarainen M, Albertsson AC, Södergård A (2011) From lactic acid to poly(lactic acid) (PLA): characterization and analysis of PLA and its precursor. Biomacromolecules 12:523–532
42. Stoclet G, Seguela R, Lefebvre JM, Li S, Vert M (2011) Thermal and strain-induced chain ordering in lactic acid stereocopolymers: influence on the composition in stereomers. Macromolecules 44:4961–4969
43. Shin EJ, Jones AE, Waymouth RM (2012) Stereocomplexation in cyclic and linear polylactide blends. Macromolecules 45:595–598
44. Hosoda N, Lee EH, Tsujimoto T, Uyama H (2013) Phase separation-induced crystallization of poly(3-hydroxybutyrate-*co*-hydroxyvalerate) by branched poly(lactic acid). Ind Eng Chem Res 52:1548–1553
45. Tsuji H, Aratani T, Takikawa H (2013) Physical properties, crystallization, and thermal/hydrolytic degradation of poly(L-lactide)/nano/micro-diamond composites. Macromol Mater Eng 298:1149–1159
46. Ishimoto K, Arimoto M, Ohara H, Kobayashi S, Ishii M, Morita K, Yamashita H, Yabuuchi N (2009) Biobased polymer system: miniemulsion of poly(alkyl methacrylate-*graft*-lactic acid)s. Biomacromolecules 10:2719–2723

47. Ishimoto K, Arimoto M, Okuda T, Yamaguchi S, Aso Y, Ohara H, Kobayashi S, Ishii M, Morita K, Yamashita H, Yabuuchi N (2012) Biobased polymers: synthesis of graft copolymers and comb polymers using lactic acid macromonomer and properties of the product polymers. Biomacromolecules 13:3757–3768
48. Okuda T, Ishimoto K, Ohara H, Kobayashi S (2012) Renewable biobased polymeric materials: facile synthesis of itaconic anhydride-based copolymers with poly(L-lactic acid) grafts. Macromolecules 45:4166–4174
49. Morita K, Yamashita H, Yabuuchi N, Hayata Y, Ishii M, Ishimoto K, Ohara H, Kobayashi S (2011) Application of star-shaped poly(lactic acid)s to two component and UV-curable coatings. J Netw Polym Jpn 32:192–196
50. Morita K, Yamashita H, Yabuuchi N, Hayata Y, Ishii M, Ishimoto K, Ohara H, Kobayashi S (2011) Synthesis of star-shaped oligomeric lactic acids with reactive double bonds and their application to UV curable coatings. Rad Tech Asia: Proc 126–129
51. Morita K, Yamashita H, Yabuuchi N, Ishii M, Arimoto K, Ishimoto K, Ohara H, Kobayashi S (2015) Anti-hydrolysis performance of cured coating films of acrylic polyols with pendant poly(lactic acid)s. Prog Org Coat 78:183–187
52. Tsujimoto T, Haza Y, Yin Y, Uyama H (2011) Synthesis of branched poly(lactic acid) bearing a castor oil core and its plasticization effect on poly(lactic acid). Polym J 43:425–430
53. Uyama H, Kuwabara M, Tsujimoto T, Nakano M, Usuki A, Kobayashi S (2003) Green nanocomposites from renewable resources: plant oil–clay hybrid materials. Chem Mater 15:2492–2494
54. Uyama H, Kuwabara M, Tsujimoto T, Nakano M, Usuki A, Kobayashi S (2004) Organic–inorganic hybrids from renewable plant oils and clay. Macromol Biosci 4:354–360
55. Tsujimoto T, Kuwabara M, Uyama H, Kobayashi S, Nakano M, Usuki A (2010) Preparation and properties of green nanocomposites from epoxidized triglycerides and a modified clay. J Adhesion Soc Jpn 46:131–136
56. Tsujimoto T, Uyama H, Kobayashi S (2003) Green nanocomposites from renewable resources: biodegradable plant oils–silica hybrid coatings. Macromol Rapid Commun 24:711–714
57. Tsujimoto T, Uyama H, Kobayashi S (2010) Synthesis of high-performance green nanocomposites from renewable natural oils. Polym Degrad Stabil 95:1399–1405
58. Tsujimoto T, Uyama H, Kobayashi S, Oikawa H, Yamahiro M (2015) Green nanocomposites from renewable plant oils and polyhedral oligomeric silsesquioxanes. Metals 5:1136–1147
59. Ikeda R, Tanaka H, Uyama H, Kobayashi S (2000) A new crosslinkable polyphenol from a renewable resource. Macromol Rapid Commun 21:496–499
60. Ikeda R, Tanaka H, Uyama H, Kobayashi S (2000) Enzymatic synthesis and curing of poly(cardanol). Polym J 32:589–593
61. Ikeda R, Tanaka H, Uyama H, Kobayashi S (2002) Synthesis and curing behaviors of a crosslinkable polymer from cashew nut shell liquid. Polymer 43:3475–3481
62. Kobayashi S, Uyama H, Ikeda R (2001) Artificial urushi. Chem Eur J 7:4755–4760
63. Kobayashi S (2003) Creation of artificial urushi. Chem Today 388:28–35
64. Otsuka T, Fujikawa S, Yamane H, Kobayashi S (2017) Green polymer chemistry: biomimetic oxidative polymerization of cardanol for synthetic approach to 'artificial urushi'. Polym J (accepted)
65. Uyama H, Kobayashi S (1993) Enzymatic ring-opening polymerization of lactones catalyzed by lipase. Chem Lett 1149–1150
66. Uyama H, Takeya K, Kobayashi S (1993) Synthesis of polyesters by enzymatic ring-opening copolymerization using lipase catalyst. Proc Jpn Acad B 69:203–207
67. Knani D, Gutman AL, Kohn DH (1993) Enzymatic polyesterification in organic media—enzyme-catalyzed synthesis of linear polyesters. 1. Condensation polymerization of linear hydroxyesters. 2. Ring-opening polymerization of ε-caprolactone. J Polym Sci Part A: Polym Chem 31:1221–1232
68. Bonduelle C, Martin-Vaca B, Bourissou D (2009) Lipase-catalyzed ring-opening polymerization of the *O*-carboxylic anhydride derived from lactic acid. Biomacromolecules 10:3069–3073
69. Ohara H, Onogi A, Yamamoto M, Kobayashi S (2010) Lipase-catalyzed oligomerization and hydrolysis of alkyl lactates. Direct evidence in the catalysis mechanism that enantioselection is governed by a deacylation step. Biomacromolecules 11:2008–2015
70. Ohara H, Nishioka E, Yamaguchi S, Kawai F, Kobayashi S (2011) Protease-catalyzed oligomerization and hydrolysis of alkyl lactates involving L-enantioselective deacylation step. Biomacromolecules 12:3833–3837
71. Ohara H, Yamamoto M, Onogi A, Hirao K, Kobayashi S (2011) Optical resolution of *n*-butyl D- and L-lactates using immobilized lipase catalyst. J Biosci Bioeng 111:19–21
72. Kobayashi S, Uyama H, Suda S, Namekawa S (1997) Dehydration polymerization in aqueous medium catalyzed by lipase. Chem Lett 105
73. Suda S, Uyama H, Kobayashi S (1999) Dehydration polycondensation in water for synthesis of polyesters by lipase catalyst. Proc Jpn Acad B 75:201–206